

Article

Kohonen Neural Network Classification for Failure Process of Metallic Organic Coating in Corrosion Environment

Yuanming Xu, Junshuang Ran * and Hao Chen

School of Aeronautic Science and Engineering, Beihang University, Beijing 100191, China; xuymg@sina.com (Y.X.); Chen_hao@buaa.edu.cn (H.C.)

* Correspondence: junshuangran@buaa.edu.cn; Tel.: +86-130-5181-0855

Academic Editor: Jae Myung Lee

Received: 21 December 2016; Accepted: 14 April 2017; Published: 20 April 2017

Abstract: A deeper insight into the changing states of corrosion during certain exposure circumstances has been investigated by applying Kohonen networks. The Kohonen network has been trained by four sets of samples and tested using another sample. All the sample data were collected during accelerated corrosion experiments and the network took the changing rate of impedance of each cycle as an input. Compared with traditional classification, the Kohonen artificial network method classifies corrosion process into five sub-processes which is a refinement of three typical corrosion processes. The two newly defined sub-processes of corrosion—namely, pre-middle stage and post-middle stage—were introduced. The EIS data and macro-morphology for both sub-processes were analyzed through accelerated experiments. The classification results of the Kohonen artificial network are highly consistent with the predictions based on impedance magnitude at low frequency, which illustrates that the Kohonen network classification is an effective method for predicting the failure cycles of polymer coatings.

Keywords: coating; corrosion; EIS; Kohonen neural network; classification

1. Introduction

There is major significance in judging the state of polymer coating in service to study the coating failure process under different conditions. Electrochemical impedance spectroscopy (EIS) is considered a very powerful technique for evaluating the protective properties of polymer coatings and their degradation during exposure to corrosive environments [1–3]. The experimental EIS data can be analyzed by appropriate models (e.g., equivalent circuits (EC)) and the fitting parameters can be used to reflect coating properties as well as the corrosion reaction at the metal/coating interface, such quantities as coating capacitance, coating resistance, and double layer capacitance, etc.

However, the determination of equivalent circuits of the coating state is very complex. Different coating states are corresponding to equivalent circuits in different forms, and often an impedance spectrum has to be resolved into different equivalent circuits. Meanwhile, orders of impedance magnitudes are diverse for different coating systems. Considering this situation, some researchers proposed to make use of the minimum phase angle and its frequency [4], impedance at low frequencies [5], and phase angle at high frequencies [6] to get parameter assessment. Compared with EC models, these methods might be simple and practical way to evaluating the coating performance. However, the application data for assessment selects a local single attribute and not in global sense, which is liable to cause inevitable errors during the evaluations. Therefore, it is necessary to seek effective approaches such that all the EIS data attributes can be analyzed and evaluation errors can be minimized. Miszczyk and Darowicki [7] proposed using principal component analysis to evaluate the

multispectral impedance of a coil-coated system. Furthermore, Hosbein [8] applied the $|Z|$ area and phase area to analyze the categorization of the protective coatings.

At the end of the last century, the artificial neural networking began to take shape in coating research. In view of the development of neural networks and the complexity of EIS, it becomes a direction for many researchers to explore the application of neural networks for the analysis of coating failures. Scholars were committed to combining neural networks with other technologies, such as expert systems [9] and fuzzy logic [10], in order to deduce the final prediction in a readily usable form. Their artificial neural network system was built by polarization test data to predict the corrosion on the metal surface. References [11,12] illustrate the utility of neural network in corrosion prediction and suggest that they may play a key role in predicting coated component life in service based on the EIS method. After that, some researchers [13] applied SOM networks to conduct an investigation on the deterioration process of organic coatings. Some other studies [14,15] have predicted some parameters such as corrosion rate and pit growth by intelligent systems, and their research illustrated that artificial neural networks are a powerful tool in predicting corrosion rate and effectively modeling maximum pit dimensions. Xu et al. [16,17] selected the changing rate of impedance and phase angle at high frequency as the training sample for SOM network, and the coatings with different breakage degrees were divided into three levels. In this paper, the coating failure process is investigated through further classification into five sub-processes by using the Kohonen artificial network, which is a refinement compared to the traditional three-stage corrosion identification.

2. Experimental Methods

2.1. Experimental Materials

High strength steel (30CrMnSiNi2A) plates were employed as metallic substrates, and dimensions of the test specimens are $40 \times 20 \times 3$ mm. The substrate was polished with emery paper to remove mill scale, cleaned with acetone and de-ionized water, and then dried prior to the coating process. Experimental data was based on the organic coating with the following surface treatments. Shot peening is the first operation. Then, a zinc layer is sprayed at a thickness of 30~60 μm . H06-076 primer type is chosen, an epoxy zinc-rich anti-corrosive primer, with a thickness of 10~25 μm and a gray color. The enamel layer is 881-Y01, a polyurethane top coat, with 40~60 μm of thickness and a blue color. The specimens were allowed to cure at room temperature and humidity for a week before exposure to an accelerated corrosion environment.

2.2. Corrosion Testing

Accelerated life testing was used in this experiment. The process of the test was to impose repeatable, measurable stresses to specimens, and these imposed stresses did not cause the change of the mechanism of corrosion protection to failures from those seen in normal use of the coating. Test specimens were exposed to the following accelerated corrosion environments during each cycle:

- Exposure to UV radiation at (60 ± 10) W/m^2 radiation intensity with a temperature of 55 °C for 24 h;
- Thermal shock test at 149 °C with heating for 10 to 15 min, and insulating for 1 h;
- Immersion in salt spray sodium chloride solution with a pH value of 4 at 40 °C for 85 h.

The time of one cycle was five days, and the total number of cycles was 14. EIS measurement was carried out at the end of each cycle.

2.3. EIS Measurement

The electrochemical measurements made use of a conventional three-electrode arrangement and a PARSTAT 2273 electrochemical impedance measuring system in the salt fog test. The reference electrode is a glass rod and the auxiliary electrode is a graphite electrode. The electrochemical cell was placed inside a shield cage in order to reduce external influence on the studied system. The experimental

data used in this paper was obtained at open circuit potential with a 10 mV sine perturbation, and the measuring frequency range was from 0.01 Hz to 100 kHz. The software used to acquire and analyze the data allows the representation of data in terms of Bode (logarithm of the impedance modulus $|Z|$ as a function of the logarithm of the frequency f) plots.

3. Experimental Results and Analysis

3.1. Morphological Analysis

The typical images of specimens experiencing different cycles are shown in Figure 1, which includes the early stage, middle stage, and late stage according to traditional classification of polymer coating quality using EIS [18] in Figure 1. As can be seen from the picture shown in Figure 1a, in the early stage, specimens did not change obviously, and the period of this stage is from the zeroth cycle to the fifth cycle. The color of the organic coats changes obviously from the sixth cycle to the ninth cycle shown in Figure 1c. Corrosion bubbling appears in part of the specimen visually and it can be observed in the phenomena of white corrosion forming flow marks, and this period corresponds to the middle stage. After the ninth cycle, it is the late stage shown in Figure 1e. The number of corrosion bubbles increases and the size of these bubbles grows obviously, even showing sunken features, as well as the white corrosion products which are formed by etching the Zn layer. During this period of corrosion, all these show that bonding force between paint and the substrate significantly decreased. In other words, the ability of the paint to prevent corrosion medium from entering into the substrate has been seriously diminished.

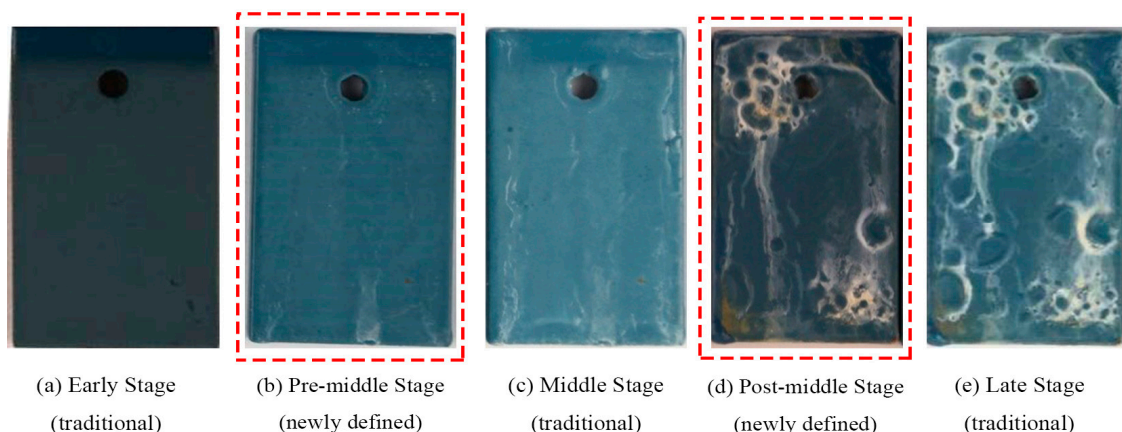


Figure 1. Five sub-processes of coating failure in macro-morphology.

A better understanding of the organic coating failure can be characterized by the following five sub-processes in terms of corresponding coating corrosion phenomena:

Early Stage: This is the initial stage of immersion and coating has good protective properties. The appearance of the coating showed in Figure 1a shows little change compared with the state before corrosion;

Pre-middle Stage: Corrosive media infiltrates the paint film gradually with an electrochemical reaction taking place, and the coating surface is still in good condition showed in Figure 1b. However, the change of color in the coating is visible to the naked eye;

Middle Stage: Moisture content in the coating is close to saturation and micro pores appear as shown in Figure 1c. It tends to peel off in coating as a result of poor protection performance and small bubbling defects can be observed on the small scales;

Post-middle Stage: The number of bubbles increases and the size of these bubbling defects grows. It turns out to be local non-protective, which is showed in Figure 1d;

Late Stage: Coating shows big flaws and is completely ineffective as shown in Figure 1e. The coating peels off totally in this stage.

It is proposed here that the two newly defined additional sub-processes—namely, the pre-middle stage and post-middle stage—are defined around the middle stage. The pre-middle stage is an unsaturated infiltration state in which the color of the organic coats changes gradually. In the middle stage, moisture content is close to saturation but coatings still have global protective properties, and it tends to peel off in coating. In the post-middle stage, coatings lose local efficacy, while coatings are entirely ineffective in the late stage.

The advantage of five sub-processes is that they can provide more information about the coating failure process and reflect detailed information of coating samples during the entire corrosion process. However, equivalent circuits of the five stages cannot be built appropriately. The five sub-processes proposed here are mainly for the purpose of Kohonen artificial network application.

3.2. Electrochemical Impedance Spectroscopy Analysis

The impedance data were considered to contain 10 points per decade of frequency for a total of 50 points which were equally spaced on a logarithmic scale. The analysis of electrochemical impedance spectroscopy was performed using the logarithm of the impedance modulus $|Z|$ ($\Omega \cdot \text{cm}^2$). Taking sample #0 for example, the fitting impedance spectroscopy of the sample #0 is shown in Figure 2.

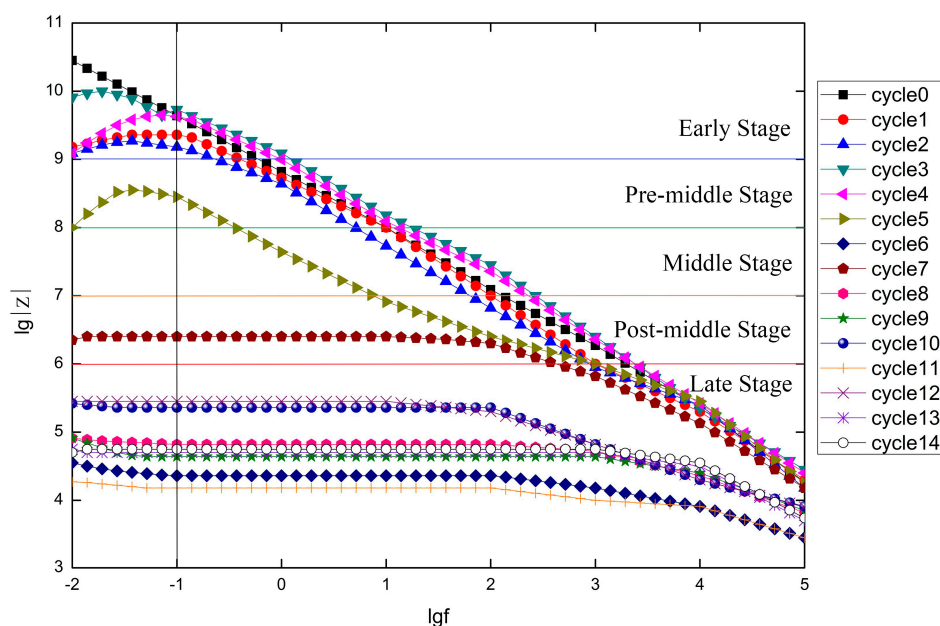


Figure 2. Electrochemical impedance modulus of sample #0.

From the zeroth cycle to the fifth cycle and low to high frequency, impedance modulus as a whole is a violently downward trend. The impedance modulus $|Z|$ of the first four cycles at the low-frequency (0.1 Hz) displays very high values ($>10^9 \Omega \cdot \text{cm}^2$). This suggests that coating as a shield can isolate corrosive media, protecting the metal from corrosive action in early immersion. As the time elapsed, the electrolyte solutions gradually penetrate the organic coating. From sixth cycle, $|Z|$ mainly declined first, and then levelled out, subsequently following a downward trend until the ninth cycle. This phenomenon shows that electrolytes will soon penetrate and create pores on the coating, exposing the metal surface. At this time, corrosion has already emerged on the metal substrate with a small area. Simultaneously, the impedance modulus values $|Z|$ at the low-frequency are in the range of $10^6 \sim 10^8 \Omega \cdot \text{cm}^2$. After that, $|Z|$ presents like a platform first, and then drops dramatically. Meanwhile,

$|Z|_{0.1\text{Hz}}$ waves around $10^5 \Omega\cdot\text{cm}^2$. At this stage, the protective performance of coating is greatly reduced and corrosion is increasingly serious. The coating has completely lost its protective ability.

The ongoing changes of the impedance module at low-frequency indicate that the protective performance of the organic coating system gradually decreased with increase of corrosion time, which might be due to the corrosion medium penetrating the organic coating to coating/metal interface bit by bit and the coatings have expired when metal corrosion reaction begins.

Reference [14] automatically classified polymer coating quality into three stages using artificial neural networks. The three groups of training data as $\log |Z| - \log f$ plots are defined as 'good', 'intermediate', and 'poor'. For the 'good' coating, the impedance modulus values in 0.1 Hz are greater than $10^9 \Omega\cdot\text{cm}^2$ and the plots approximate a tilted straight line, while for the 'intermediate' coating the data curves maintain a straight level for a short distance then decline sharply, and the impedance modulus values in 0.1 Hz are in the range of $10^6 \sim 10^8 \Omega\cdot\text{cm}^2$. For the 'poor' coating, the data is about $10^6 \Omega\cdot\text{cm}^2$ even much less. Based on this reference, it can be considered that cycles 0 to 4 of sample #0 are in the 'good' stage, while cycles 5 and 7 are in the 'intermediate' stage and cycles 8 to 14 are in 'poor' stage. According to the experimental data of five sub-processes of the coating failure which are already proposed in the morphological analysis in Section 3.1, approximate orders of the impedance modulus values in 0.1 Hz of each stage are shown in Figure 2.

4. Kohonen Artificial Network Method for Coating Corrosion Prediction

The Kohonen artificial network is applied to analyze the impedance spectrum directly, which avoids the choice of equivalent circuit. The network consists of two layers of neurons ordered in a low-dimensional map, a linear array of artificial neurons. In the second layer, five neurons represent the five stages of the coating degradation process. KNN is a kind of intelligent non-supervised learning network with no prior information about cluster existence in input samples during the training process. Such self-organizing capability of the Kohonen network allows users to assume that all the samples in the same node or in its surroundings are similar according to the features being evaluated.

The Kohonen network method can be used effectively to analyze EIS data for study of the coating failure process. Coating failure begins with a local defect, but EIS cannot reflect such local information. As a result, coating failure cycle cannot be accurately judged in time. Kohonen network can not only divide the coating corrosion process into three sub-processes according to the traditional classification, but also classify the deterioration process into five stages, which can reflect the changing process of the coating protection in more detail. Because of this flexibility, further evaluation of protective properties of the organic coating can be made. Another obvious advantage is that the impedance data points used in training and testing are corresponding to multiple frequencies instead of a single frequency 0.1Hz, which can avoid evaluation errors to the least extent.

4.1. The Changing Rate of Impedance

According to the reference [19,20], the selection of the form of input data is very important for classification results. Compared with other EIS parameters, such as coating resistance, coating capacitance, polarized resistance, and double-layer capacitance, etc., the changing rate in impedance which satisfies Equation (1) can reflect the changing process of the impedance more sensitively in the entire frequency range and can help to recognize the features of the deterioration process more clearly. The parameter $k(f)$ expressed in differential form can probably intensify the characteristics of each stage in the frequency range. Therefore, for classification purposes, the failure stages of the coating can be distinguished effectively which does not require building EC and analyzing other parameters.

$$k(f) = \frac{\log|Z_{f_i}| - \log|Z_{f_{(i-1)}}|}{\log f_i - \log f_{(i-1)}} \quad (1)$$

4.2. Structure and Procedure of the Kohonen Artificial Network

The structure of Kohonen artificial networks is a kind of feed forward neural networks, including an input layer and a competitive layer which is also called output layer. The neurons are highly interconnected to each other. The variable weights connect the neurons of the input layer and the competition layer. The topology map of the Kohonen artificial network adopted in this research is showed in Figure 3, which defines an ordered mapping.

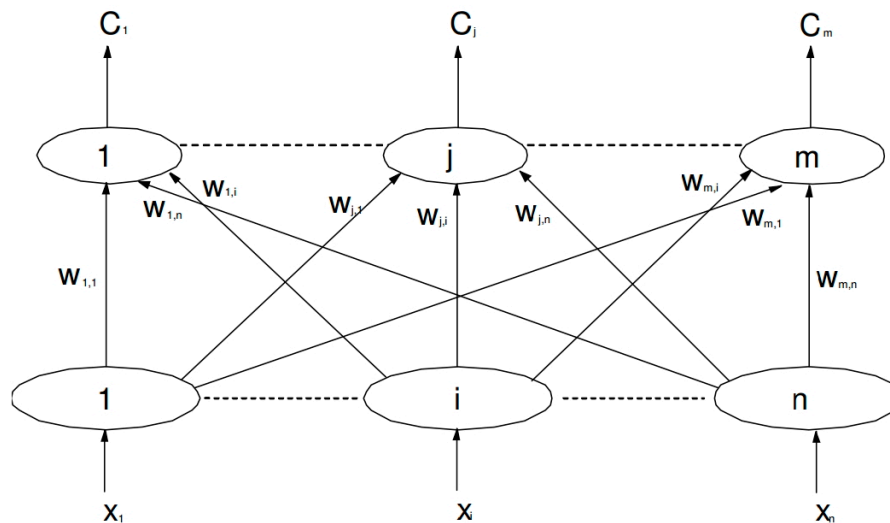


Figure 3. The topology map of one-dimensional KNN.

In the input layer, the number of neurons of the neural network, is consistent with the dimension of input samples. Since the analysis of EIS data recorded 50 points on a logarithmic scale ranging from 0.01 Hz to 10^5 Hz in the experiment and the resulted changing rate of impedance modulus $k(f)$ of each cycle was calculated, the dimension of the input sample is determined as 49. The second layer is the competitive layer in which neurons are distributed in one-dimension in our research and the number of neurons in this layer is set to five corresponding to five sub-processes of the organic coating failure process. In such a one-dimensional competitive layer, neurons will be arranged in a straight line. The less difference samples have on the line, the much closer the positions of neurons stimulated by the samples will be. Therefore, according to the positions of superior neurons in the competitive layer, the change trend of coating stages can be observed easily.

The process of predicting the experimental data period using the neural network model is divided into two steps. The first step is to classify the coating data to be predicted, and this process is divided into network training and testing. During the training process, each input datum x_s is presented to the neural network. Only the neuron whose weight vector is most similar to the input vector x_s is stimulated and this process is so called competitive learning. The specific steps of training procedure of the network are illustrated as follows:

1. Initialize the network by randomly selecting network weights.
2. Calculate the changing rate of impedance modulus $k(f)$, which is the slope curve points of the impedance curve of amplitude-frequency in Bode diagram, and present to the network.
3. Track the best matching unit (BMU) which produces the smallest Euclidean distance Equation (2) between the input vector and the weight vector of neurons in the second layer.

$$Ed = \min_j \left\{ \sum_{i=1}^{49} (x_{si} - \omega_{ji})^2 \right\}, j = 1, 2, \dots, 8 \quad (2)$$

where x_{si} and ω_{ji} are the i th coordinate of the input data x_s and the i th weight of neuron j in the second layer, respectively.

4. The radius of the neighborhood of the BMU is calculated which starts initial large value r_0 of 2.5. According to Equation (3), the radius of the network diminishes in each time-step.

$$r(t) = r_0 e^{-t/\lambda} \quad (3)$$

where r_0 is the initial radius of the network; t is the current iteration and λ is the time constant calculated by Equation (4).

$$\lambda = \frac{N}{R} \quad (4)$$

where N is the number of iterations and R is the radius of the second layer.

5. Adjusting the nodal weights of the BMU and weights of other nodes within the radius of the BMU by Equation (5).

$$\omega_{ij}(t+1) = \omega_{ij}(t) + \eta \left(1 - \frac{d_r}{d_{\max} + 1} \right) [x_{si} - \omega_{ij}(t)], d_r = 0, 1, \dots, d_{\max} \quad (5)$$

where η is the learning rate; $\omega_{ij}(t)$ is the numerical value of the weight ω_{ij} at the previous iteration. The size of d_{\max} , which at the beginning of learning covers the whole neural network, decreases during the training process and finally the value is zero. The learning rate η is one of the important parameters and is also changing during the training by Equation (6).

$$\eta = (\eta_{\text{initial}} - \eta_{\text{final}}) \left(1 - \frac{n_{\text{previous}}}{n_{\text{total}}} \right) + \eta_{\text{final}} \quad (6)$$

6. Determine whether the algorithm ends, if not, return to step 2.

4.3. Application of the Kohonen Artificial Network

4.3.1. Sample Training

An unsupervised competitive learning method is used for sample training, which means that it just simply provides samples to the network without supplying an ideal output. Four sets of samples from Sample 1 to Sample 4, of which the fitting impedance modulus spectra and the parameter $k(f)$ are shown in Figures 4 and 5, are used for sample training. The training should be split into two phases. Phase 1 will reduce the learning rate from 0.1 to 0.04, and the neighborhood radius from half the length of the second layer to the immediately surrounding neurons. Phase 2 will over double the number of iterations in Phase 1. In Phase 2, the learning rate will be reduced from 0.04 to 0.01, and the neighborhood radius value will remain fixed at 1, which means the BMU is the only neuron to be altered. Analyzing these parameters, Phase 1 allows the network to divide the space roughly, and Phase 2 performs the fine-tuning of the KNN to a more accurate representation.

The sample training has been completed when classification results tend to be stable and five sub-processes become clear. Impedance modulus data at 0.1 Hz of the four samples and stages corresponding to each cycle classified by the $|Z|_{0.1\text{Hz}}$ can be found in Figure 4. The ranges of $|Z|_{0.1\text{Hz}}$ of five sub-processes can be clarified after collecting and organizing these data. The training results can make the failure stages of coating more refined, and it indicates that the Kohonen artificial network is an effective method in the study of coating failure states.

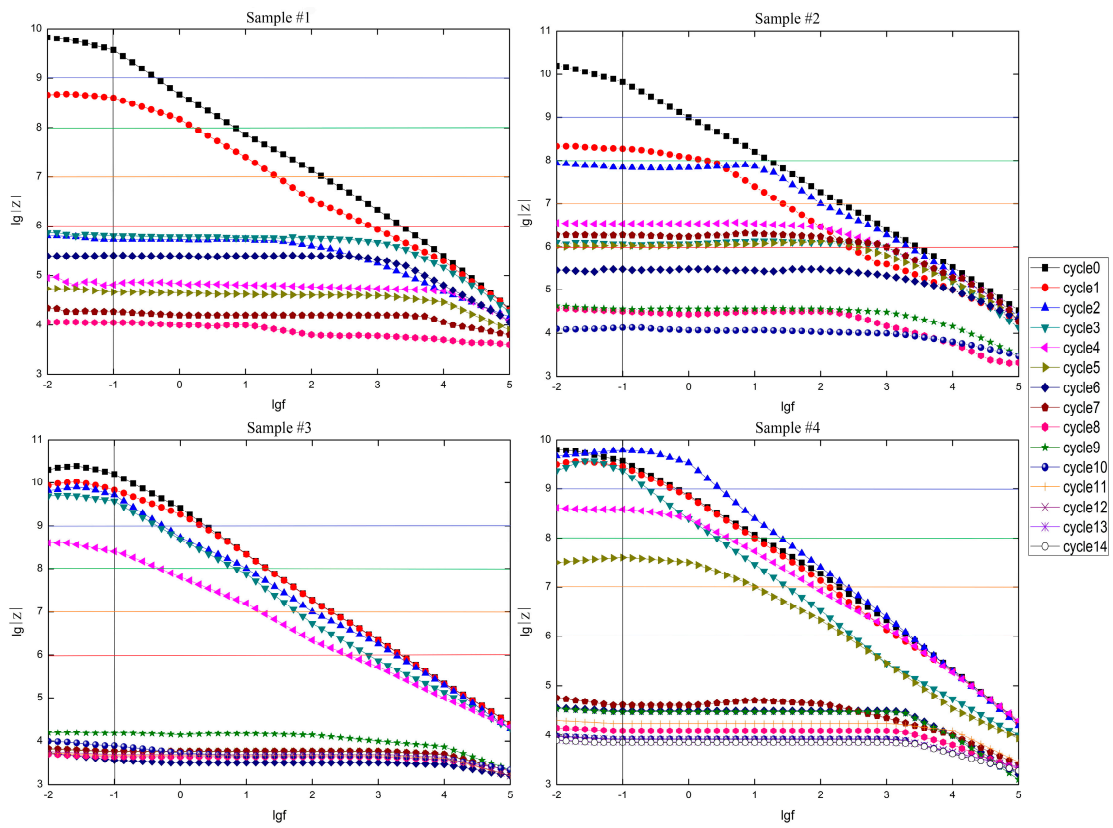


Figure 4. Impedance modulus spectrums of training samples.

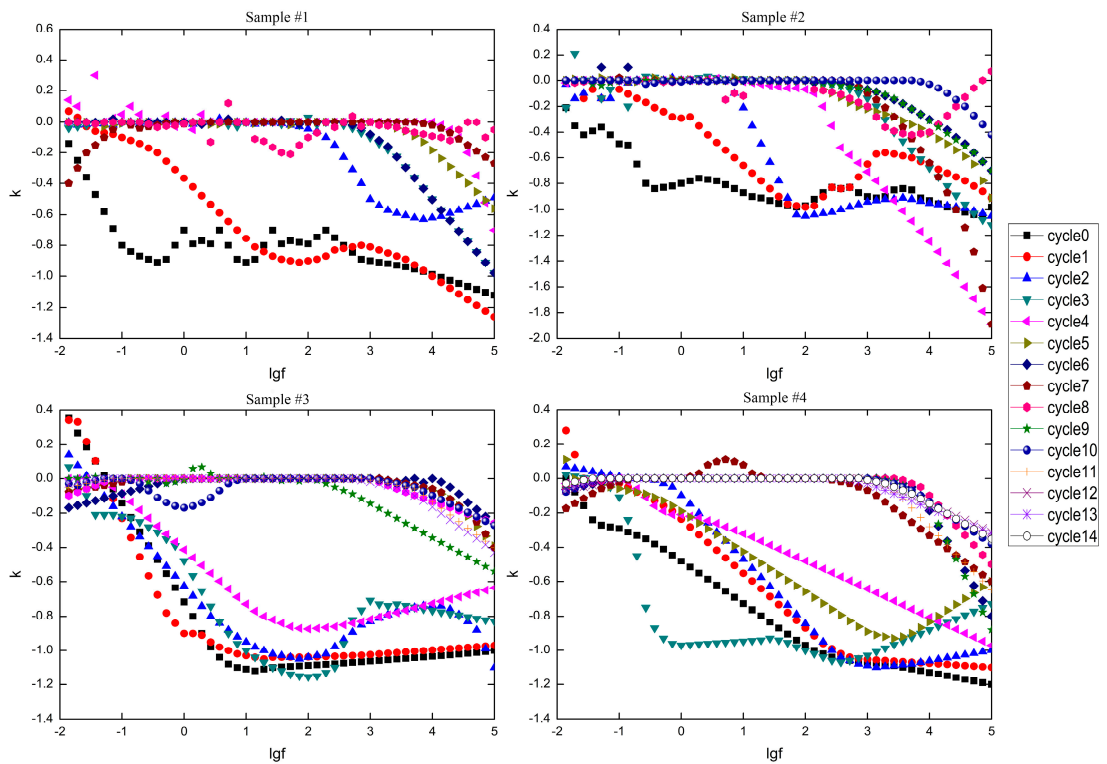


Figure 5. The parameter $k(f)$ of training samples.

4.3.2. Sample Testing

The trained Kohonen network can be utilized to predict the failure process of other coating samples, i.e., test samples which did not participate in the training process. The test sample data has to have the same format as the training sample data, i.e., containing 49 inputs. The experimental Sample 0 analyzed in Section 3 is selected as the test sample, of which the fitting impedance modulus data and the parameter $k(f)$ are shown in Figures 2 and 6 separately. In line with the fitting data of the impedance modulus and the impedance modulus slope, it is able to obtain classification results and forecast a failure state in different periods of the sample during the corrosion process.

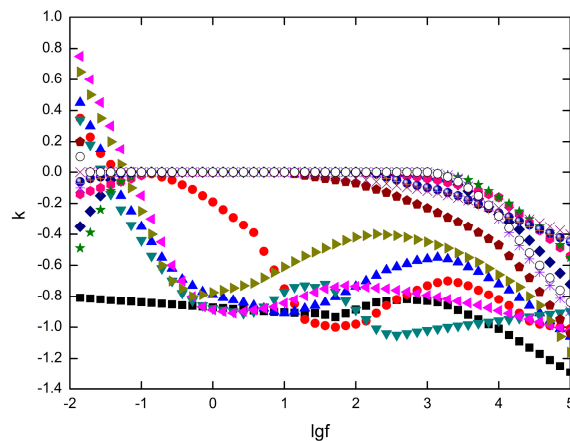


Figure 6. The parameter $k(f)$ of Sample 0.

Classification results based on KNN and $|Z|_{0.1\text{Hz}}$ are shown in Figure 7. For the classification of KNN, first four cycles are classified to Sub-process 1 in which the coating has good protective properties. The period from the 5th cycle to the 11th cycle includes Sub-process 2, Sub-process 3, and Sub-process 4, showing the refinement compared to traditional classification by the Kohonen artificial network. After the 11th cycle, the coating corrosion process is in Sub-process 5. A jump phenomenon appears in the 9th cycle because of self-healing behavior occurring when corrosion happens. Corrosion products jammed the pores of the coating, obstructing medium infiltration [20]. This phenomenon can also be seen in impedance spectroscopy.

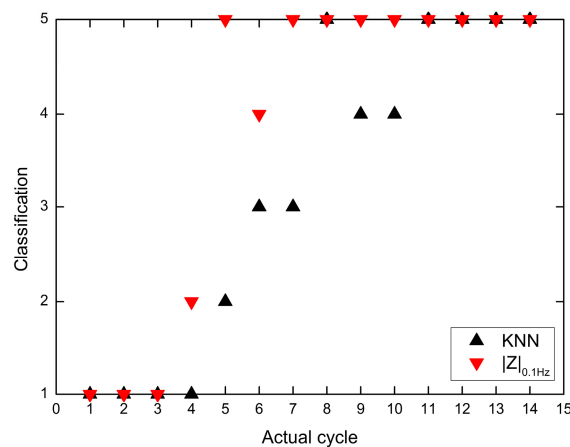


Figure 7. Classification results of Sample 0.

According to the morphological analysis in Section 3.1, it can be concluded that the classification of the Kohonen network is more accurate than that of $|Z|_{0.1\text{Hz}}$. In an actual project, the coating will be

repaired at the middle stage, which corresponds to the Sub-process 3. Hence, accurate assessment of corrosion stage of the coating is necessary for coating life estimate. It can be observed in Figure 7 that the coating will be judged to be failure prematurely based on $|Z|_{0.1\text{Hz}}$. By contrast, the application of KNN is more reliable.

In order to forecast cycles, the Euclidean distance between the cycles of testing Sample 0 and the trained samples were calculated after classification. Taking the third cycle of Sample 0 in Table 1 for example, the shortest Euclidean distance between the third cycle of Sample 0 and the trained sample appears at Cycle 2, which means that the forecast result of Cycle 3 of Sample 0 is Cycle 2. In this way, it is easy to obtain every forecast cycle of Sample 0 shown in Figure 8.

Table 1. Selecting forecast cycle for the third cycle of Sample 0.

Cycles of Training Sample 0	Euclidean Distance
1	0.56
2	0.37
3	0.85
4	2.34
5	8.30
6	11.98
7	12.21
8	20.01
9	20.42
10	14.23
11	20.13
12	13.84
13	17.89
14	19.77

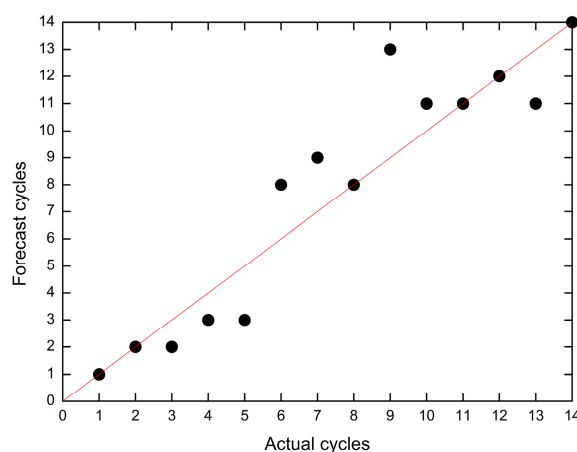


Figure 8. Forecast cycles of Sample 0.

Because of the individual differences of training samples, the coating corrosion rate of each sample is not the same. The corrosion rates of Samples 1 and 3 are too fast to capture Sub-process 3 and Sub-process 4. The corrosion Stage 4 of Sample 4 is also not successfully captured. The jump phenomenon of Sample 2 occurs at the seventh cycle, which is not the same as the test sample, and the self-healing behaviors of other samples are not acquired. As a result, the forecast cycle of the jump point of the test sample, which is the ninth cycle, is inaccurate. However, the other forecast cycles are basically consistent with the actual cycles, of which error cycles mostly are less than two cycles. This illustrates that the refinement of coating corrosion process can be obtained effectively by the Kohonen artificial network. In other words, the coating deterioration is presented more clearly by using the KNN combined with the EIS method, corrosion cycles can be predicted accurately.

5. Summary and Conclusions

In this paper, the possibility of using a self-organizing Kohonen classification network as a prediction tool for analysis of coating failure stages is reported. In particular, the challenging feature that has been proposed for such intelligence-based assessments of coating corrosion deterioration appears to be the refinement of traditional three stages of the corrosion process into five sub-processes. The KNN can effectively classify the samples, and provide judgments of corrosion sub-processes as well as forecast the corrosion cycles, which can be helpful in further analysis of coating failures along with EIS methods. The great advantage of KNN analysis is that the points of EIS data on a multiple frequency scale are used for training and testing, which can avoid evaluation errors to the least extent. In our study, we have found that the KNN classification assisted by EIS data appears to provide reasonably interpretable results more easily than only EIS analysis.

More in-depth research needs to be done. Further studies should be carried out in order to investigate the use of samples in a more effective way from each category necessary for building a reasonable class model for improving accuracy. Study of the classification of coating degradation based on multiple attributes is a good research direction.

Acknowledgments: This research was supported by the National High Technology Research and Development Program of China (863 Program), the Aeronautical Science Foundation of China (2014ZE21009), and the Foundation of the Key Laboratory of Beijing, China.

Author Contributions: Yuanming Xu was responsible for the experimental work and results analysis, and drafted the manuscript; Junshuang Ran and Hao Chen contributed to experimental operations and data collection; Junshuang Ran edited and revised the manuscript.

Conflicts of Interest: The authors declare no conflict of interest. The founding sponsors had no role in the design of the study; in the collection, analyses, or interpretation of data; in the writing of the manuscript, or in the decision to publish the results.

References

1. Mansfeld, F. Use of electrochemical impedance spectroscopy for the study of corrosion by polymer coatings. *J. Appl. Electrochem.* **1995**, *25*, 187–202. [[CrossRef](#)]
2. Romano, A.P.; Olivier, M.G. Investigation by electrochemical impedance spectroscopy of filiform corrosion of electrocoated steel substrates. *Prog. Org. Coat.* **2015**, *89*, 1–7. [[CrossRef](#)]
3. Hamlaoui, Y.; Pedraza, F.; Tifouti, L. Corrosion monitoring of galvanised coatings through electrochemical impedance spectroscopy. *Corros. Sci.* **2008**, *50*, 1558–1566. [[CrossRef](#)]
4. Duarte, R.G.; Castela, A.S.; Ferreira, M.G.S. Influence of ageing factors on the corrosion behavior of polyester coated systems-A EIS study. *Prog. Org. Coat.* **2007**, *59*, 206–213. [[CrossRef](#)]
5. Hack, H.P.; Matteson, M.A. Feasibility of Using Artificial Neural Networks with Electrochemical Impedance Spectroscopy Data from Coated Steel. In Proceedings of the National Association of Corrosion Engineers (NACE) Annual Corrosion Conference and Exposition: Water and Waste Water Industries, Denver, CO, USA, 24–29 March 1996.
6. Mahdavian, M.; Attar, M.M. Another approach in analysis of paint coatings with EIS measurement: Phase angle at high frequencies. *Corros. Sci.* **2006**, *48*, 4152–4157. [[CrossRef](#)]
7. Miszczyk, A.; Darowicki, K. Multispectral impedance quality testing of coil-coating system using principal component analysis. *Prog. Org. Coat.* **2010**, *69*, 330–334. [[CrossRef](#)]
8. Hosbein, K.H.; Swartz, N.A.; Clare, T.L. Electrochemical identification and categorization of the protective quality of intact and damaged coatings. *Electroanalysis* **2014**, *26*, 1935–1944. [[CrossRef](#)]
9. Rosen, E.M.; Silverman, D.C. Corrosion Prediction from Polarization Scans Using an Artificial Neural Network Integrated with an Expert System. *Corrosion* **1992**, *48*, 732–745. [[CrossRef](#)]
10. Jang, J.S.R. ANFIS: Adaptive-network based fuzzy inference systems. *IEEE Trans. Syst. Man Cybern.* **1993**, *23*, 665–685. [[CrossRef](#)]
11. Lee, C.C.; Mansfeld, F. Automatic classification of polymer coating quality using artificial neural networks. *Corros. Sci.* **1999**, *41*, 439–461. [[CrossRef](#)]

12. Kumar, G.; Buchheit, R.G. Use of Artificial Neural Network Models to Predict Coated Component Life from Short-Term Electrochemical Impedance Spectroscopy Measurements. *Corrosion* **2008**, *64*, 241–254. [[CrossRef](#)]
13. Zhao, X.; Wang, J.; Wang, Y.; Kong, T.; Zhong, L.; Zhang, W. Analysis of deterioration process of organic protective coating using EIS assisted by SOM network. *Electrochem. Commun.* **2007**, *9*, 1394–1399. [[CrossRef](#)]
14. Birbilis, N.; Cavanaugh, M.K.; Sudholz, A.D.; Zhu, S.M.; Easton, M.A.; Gibson, M.A. A combined neural network and mechanistic approach for the prediction of corrosion rate and yield strength of magnesium-rare earth alloys. *Corros. Sci.* **2011**, *53*, 168–176. [[CrossRef](#)]
15. Cavanaugh, M.K.; Buchheit, R.G.; Birbilis, N. Modeling the environmental dependence of pit growth using neural network approaches. *Corros. Sci.* **2010**, *52*, 3070–3077. [[CrossRef](#)]
16. Xu, A.; Zhang, F.; Luo, B.; Jin, F.; Zhang, T. Investigation the protective performance of organic coatings with different breakage degree using EIS united to SOM neural network. *Int. J. Electrochem.* **2013**, *8*, 1895–1902.
17. Xu, A.T.; Zhang, F.; Luo, B.; Jin, F.; Zhang, T.R. Investigation the deterioration process of organic coating using changing rate of phase angle at high frequency united to neural network. *Int. J. Electrochem.* **2013**, *8*, 773–779.
18. Cao, C.N.; Zhang, J.Q. *Introduction to Electrochemical Impedance Spectroscopy*; Science Press: Beijing, China, 2002.
19. Gao, Z.M.; Song, S.Z.; Xu, Y.H. Electrochemical impedance spectroscopy analysis of coating deterioration process with Kohonen neural networks. *J. Chin. Soc. Corros. Prot.* **2005**, *25*, 106–109.
20. Zhao, X. Characteristics of Electrochemical Impedance Spectroscopy in Deterioration Process of Organic Coating. Ph.D. Thesis, Ocean University of China, Qingdao, China, 2007.



© 2017 by the authors. Licensee MDPI, Basel, Switzerland. This article is an open access article distributed under the terms and conditions of the Creative Commons Attribution (CC BY) license (<http://creativecommons.org/licenses/by/4.0/>).